

RECENT PROTON EDM STORAGE RING DEVELOPMENTS

Richard Talman
Laboratory of Elementary-Particle Physics
Cornell University

Trento, Italy 1 October, 2012

Contents

| | | |
|---|---|----|
| 1 | Determining Proton and Neutron EDM's in an All-Electric Storage Ring | 3 |
| 2 | EDM Measurement Challenges | 4 |
| 3 | Novel Polarimetry | 5 |
| 4 | All-Electric Storage Ring Design | 6 |
| 5 | Resonant Polarimetry | 11 |
| 6 | Beam-Beam Polarimetry | 17 |
| 7 | Storage Ring Options | 19 |
| 8 | Measuring p and ${}^7\text{Li}$ EDM's in the Same Ring | 21 |
| 9 | (Precisely-) Fixed Frequency Feed-Forward Storage Ring Operation (as Contrasted with Polarimeter-RF Feedback) | 22 |

1 Determining Proton and Neutron EDM's in an All-Electric Storage Ring

- It is important to obtain the EDM's for both proton and neutron. One has to extract the neutron value using deuterons or some other complex nuclei.
- It is not typically possible to freeze the spins of a given complex nucleus in a purely electric storage ring.
- Proton beam polarization can be frozen in an all-electric storage ring. The magic β -value is $\beta = 0.6$.
- A ${}^7\text{Li}$ beam can also be frozen in an all-electric storage ring. The magic β -value is $\beta = 0.63$. But a large electric field (and/or large bend radius) is required.
- ${}^7\text{Li}$ beams are routinely polarized at TRIUMF in Vancouver, Canada.

2 EDM Measurement Challenges

- **Relative precession task:** Distinguish EDM-induced vertical precession from spurious, wrong-plane, MDM-induced, precession. For comparable deflecting fields the MDM torque exceeds the (nominal, 10^{-29} e-cm) EDM torque in the ratio 3×10^{-16} .
- **Absolute precession task:** For a pure Dirac particle in a magnetic field the precession is 2π per turn. At one microsecond per turn, this is of order 10^7 radians/s.
- Applying the 3×10^{-16} ratio, we therefore plan to measure a “nominal” EDM-induced precession of order 10^{-9} r/s.
- This is about 0.1 mr/day.

3 Novel Polarimetry

- Magnetic resonance is proposed for monitoring the beam polarization. The method is passive and non-destructive.
- The main lattice modification is the introduction of “mini-beta” sections.
- This also makes “beam-beam polarimetry” based on elastic proton-proton scattering practical.
- The beam-beam polarimeter measures transverse polarization.
- The magnetic resonance polarimeter measures longitudinal polarization. It could be called an NMR or MRI polarimeter but it is an external cavity rather than the nuclear spin that resonates.
- Shared resonators measure sum or difference of beam polarizations, $P_1 \pm P_2$.

4 All-Electric Storage Ring Design

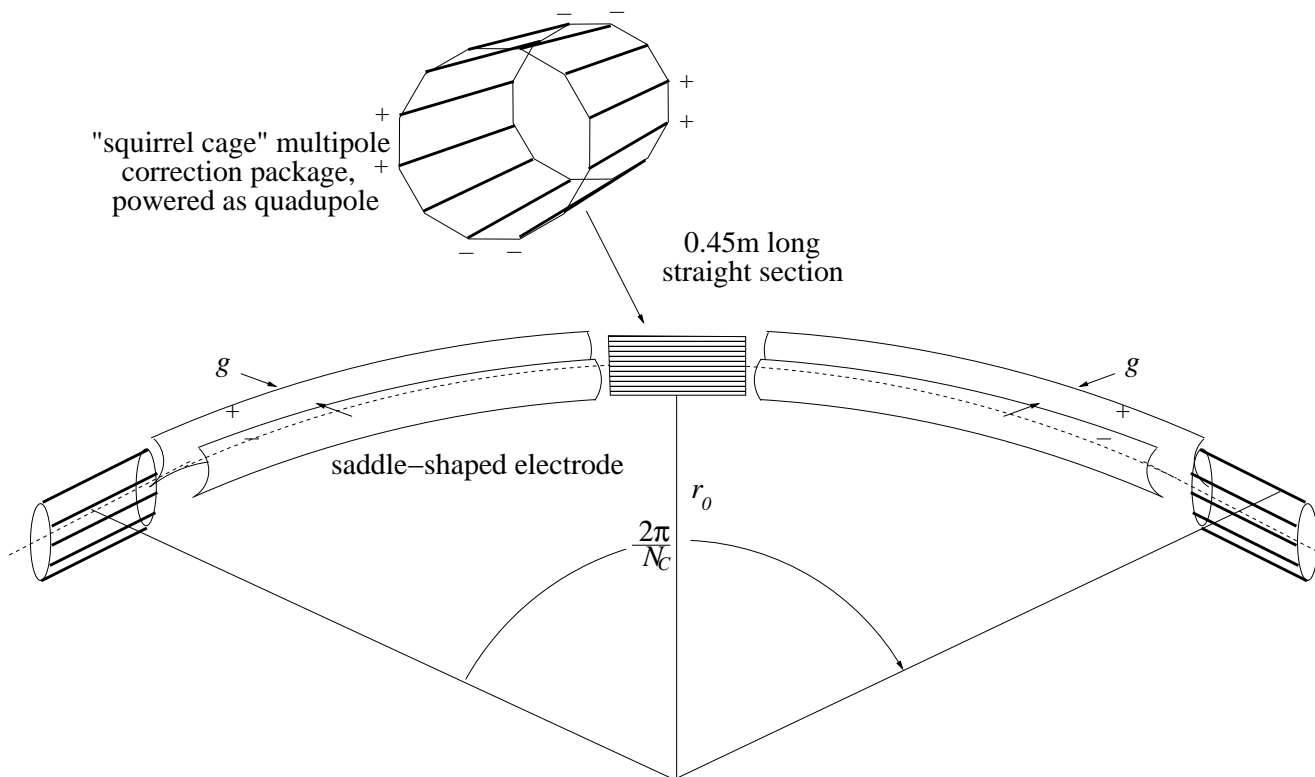


Figure 1: Sketch of one cell of baseline proton EDM lattice. There are counter-circulating proton beams.

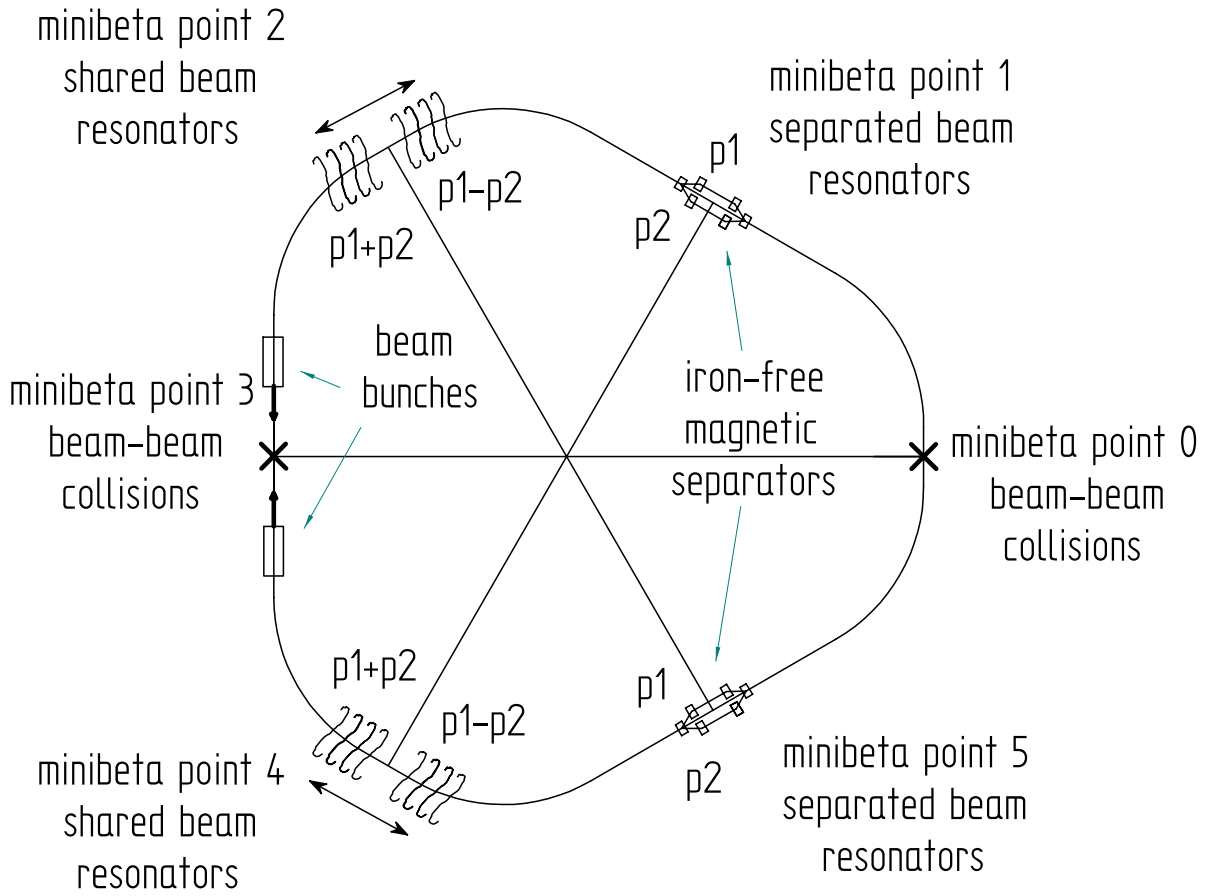


Figure 2: “Multi-Mini-beta” ring in the FNAL accumulator ring tunnel. There are polarimeters at each of the six mini-beta sections, at the centers of both long and short straight section.

4.1 Lattice and Mini-Beta Design

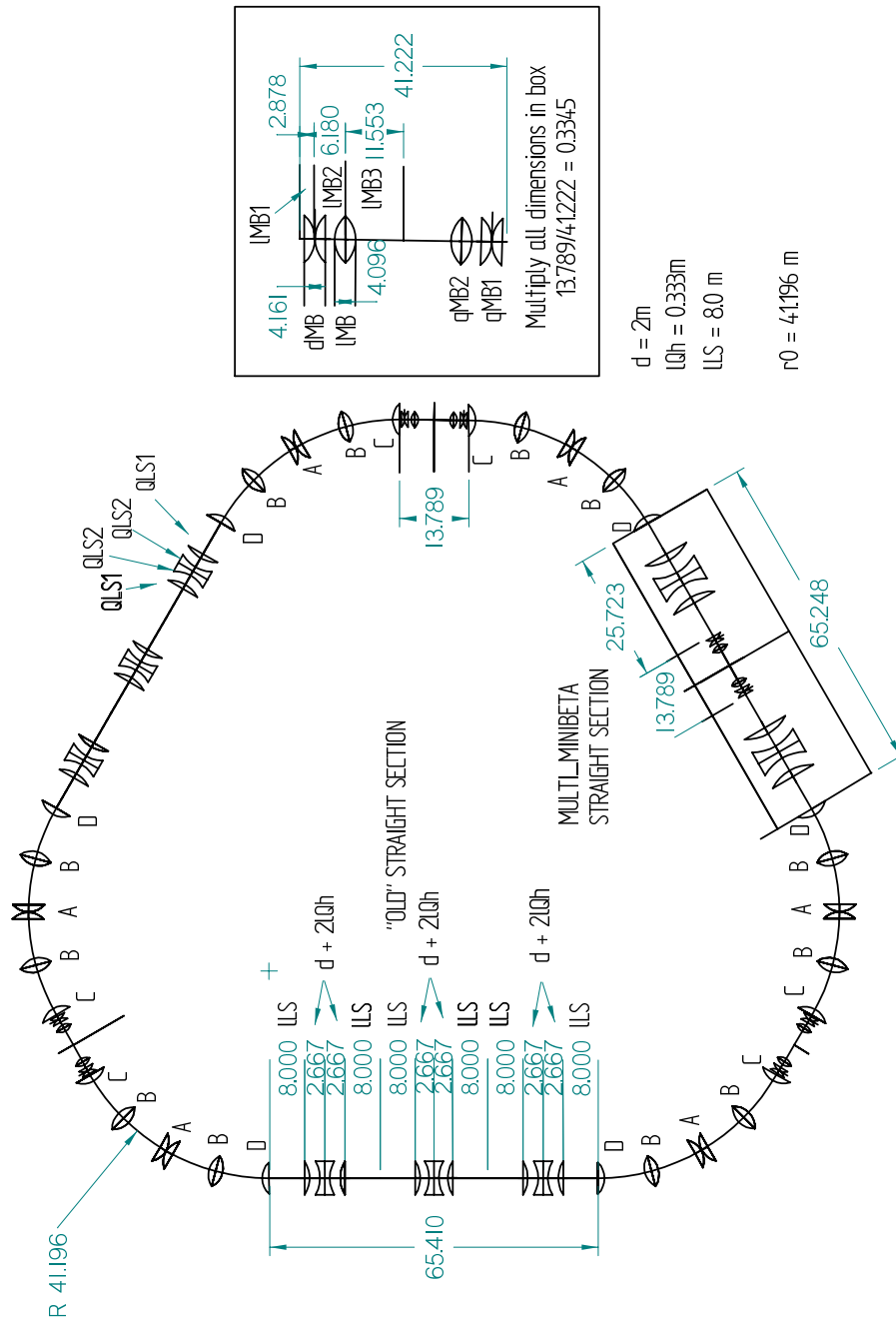


Figure 3: The “Multi-Mini-beta” proton EDM ring in the Fermilab Accumulator Ring tunnel and the ring. There is a mini-beta section at the center of each straight section

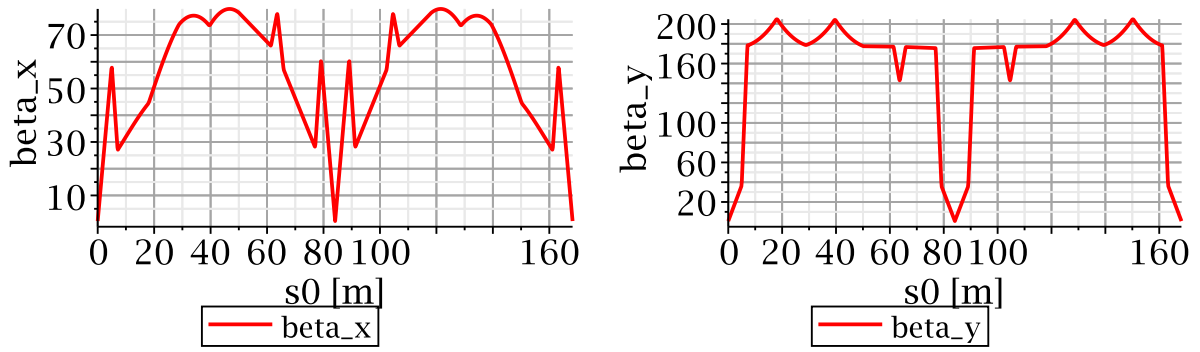


Figure 4: Plots of lattice functions for (one third of) the multi-mini-beta lattice. Vertical optics have been more carefully matched than horizontal.

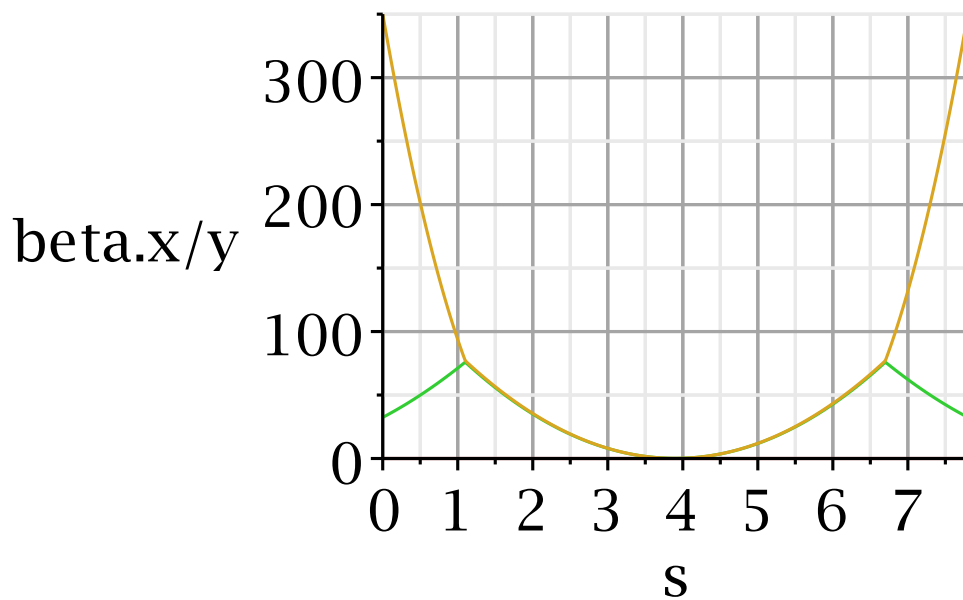


Figure 5: Beta function dependence for the six mini-beta sections. At the minima $\beta_x^* = 0.311$ m and $\beta_y^* = 0.718$ m. Though favorable for beam-beam luminosity, these values are unnecessarily small for resonant polarimetry.

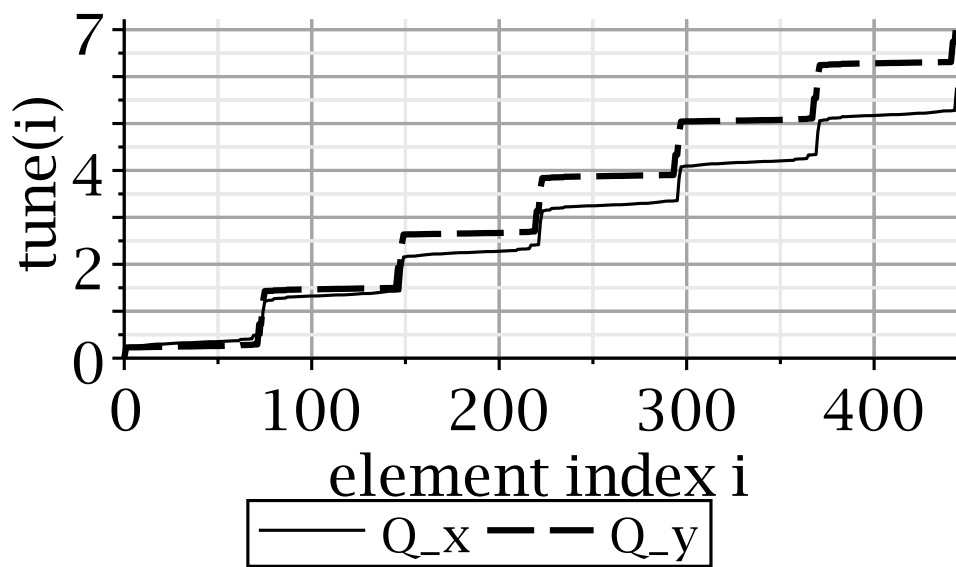


Figure 6: Advance of horizontal tune $Q_x(i)$ and vertical tune $Q_y(i)$ as the element index i advances along the central orbit. There is a tune advance of about 1 in each of the curves at each mini-beta section.

5 Resonant Polarimetry

5.1 Apparatus

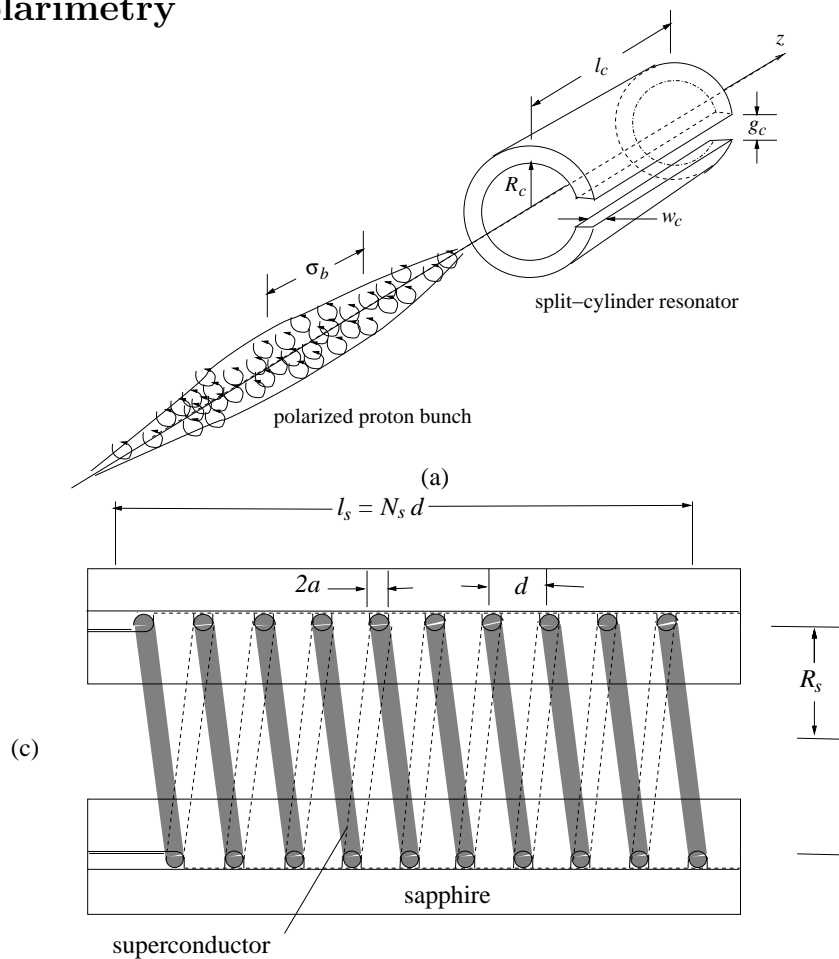


Figure 7: (a) Perspective view of the polarimeter. Dimensions are defined for the polarized proton bunch and the superconducting split-cylinder resonator. The resonator gap, shown as vacuum in the figure, may actually be filled by a low loss sapphire spacer. (c) A 30 turn solenoid gives 30 times greater signal and (estimated) signal to (thermal) noise ration comparable with the one turn solenoid.

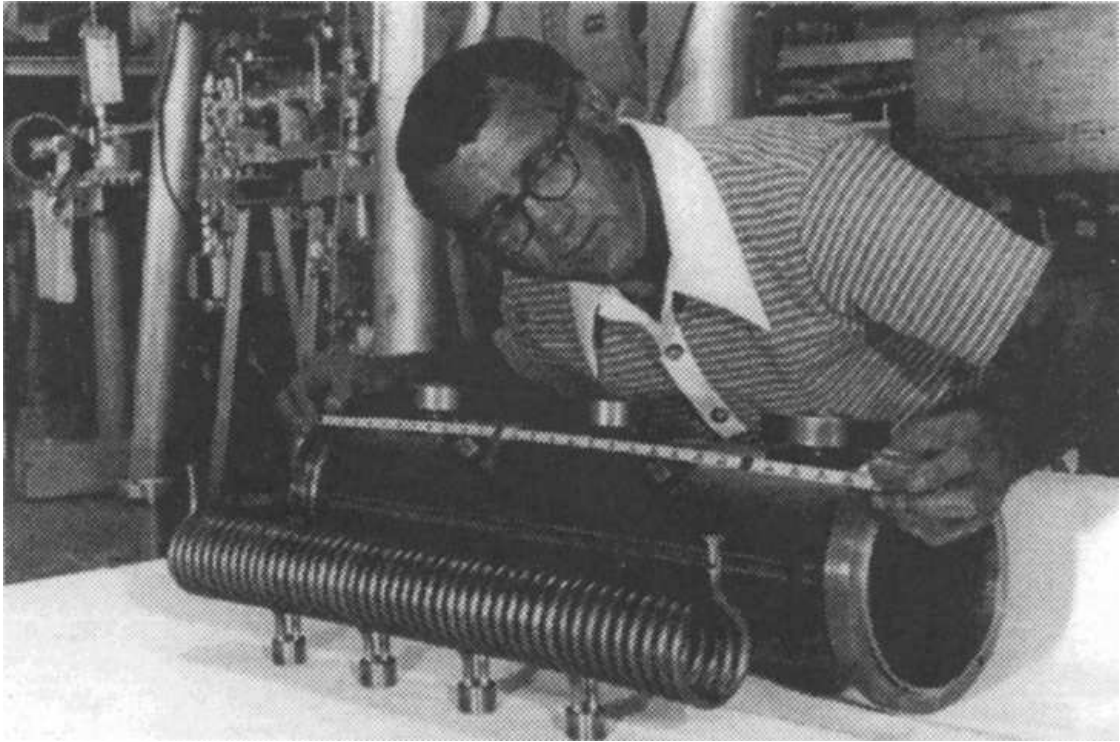


Figure 8: Helical niobium resonator developed at Argonne National Lab for heavy ion linac.

5.2 \mathcal{EMF} Induced in Loop Threaded by a Polarized Proton Bunch

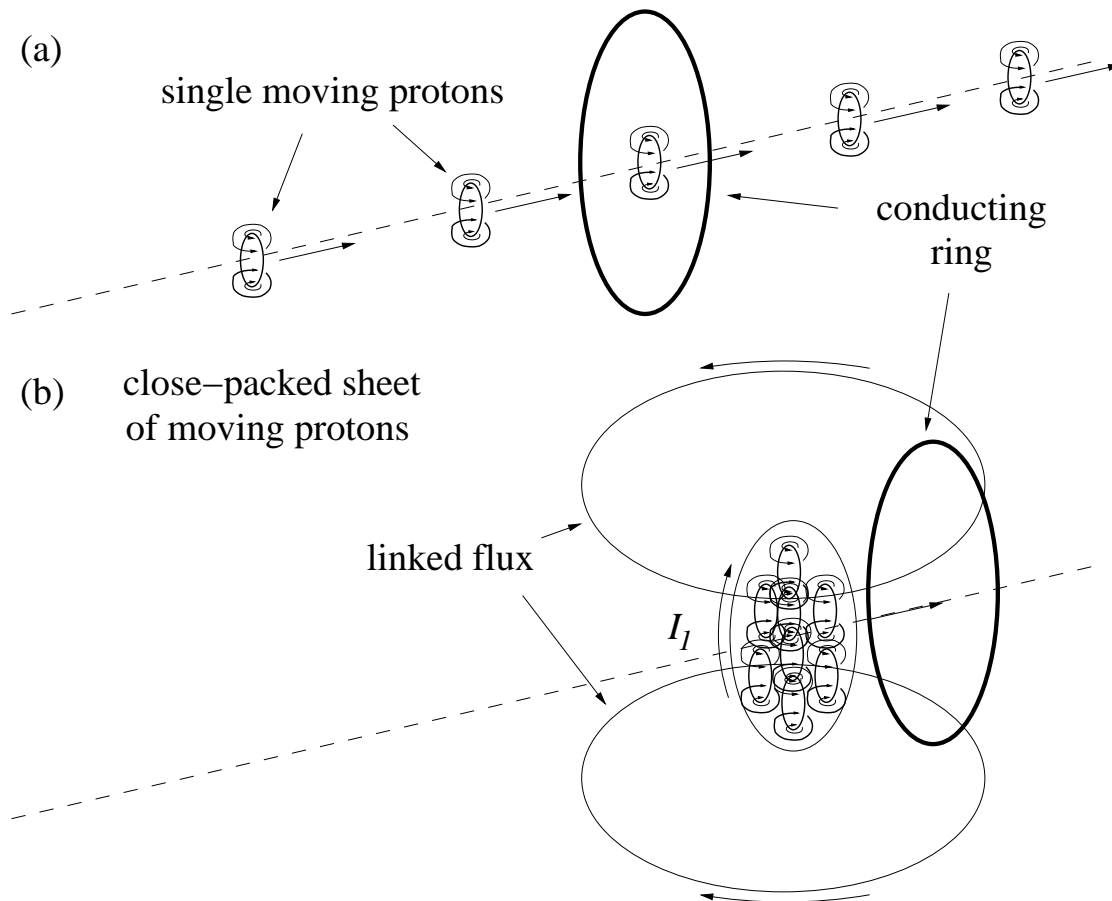


Figure 9: Protons passing through a conducting ring. The little ellipses represent proton current loops. Magnetic flux lines are indicated by little circles. In (a) there are single protons, each of radius R_1 . In (b) there are N_p protons in a closely-packed protons in a circular sheet of radius $\sqrt{N_p}R_1$.

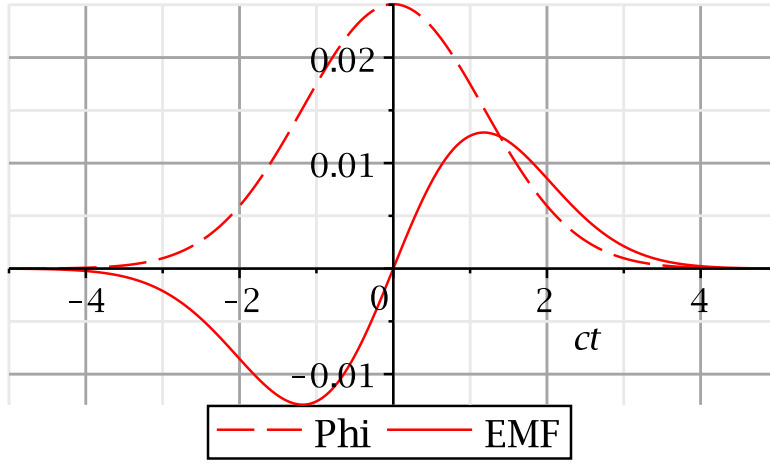


Figure 10: Plots of flux $\Phi_m(R_c, \sigma_b, ct)$ and voltage $V(ct)$ for $R_c = 0.01$ m and $\sigma_b = 1.0$ m. The absolute scale is arbitrary. The relative scale assumes $v/c = 0.6$. With ct in meters, the optimal response to such a bipolar pulse would have period $T_{\text{res}} = 4(ct)_{\text{max}}[m]/c \approx 5/c = 16.67$ ns for a frequency $f_{\text{res}} = 60$ MHz.

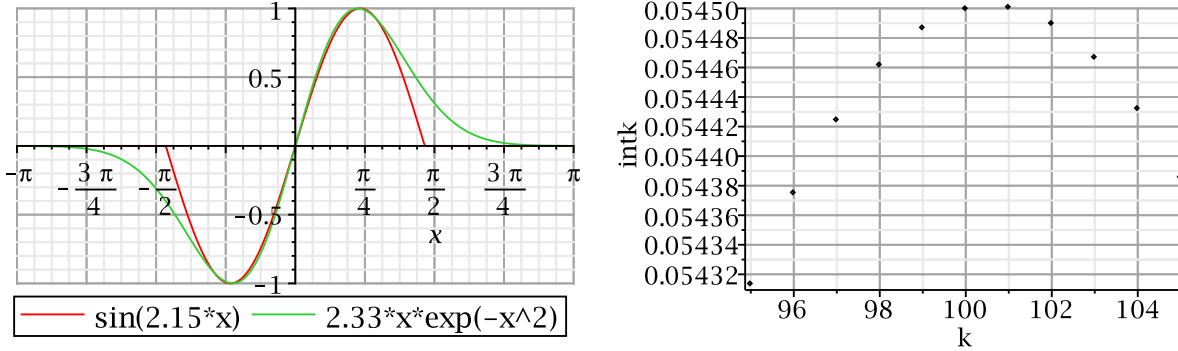


Figure 11: The left figure shows a “tolerably good” cut-off sinusoidal fit superimposed (for approximate Fourier analysis). The right hand plot shows Fourier coefficients in the Fourier expansion of the resonator excitation. The frequency spacings are equal to the revolution frequency, which here is taken to be 1 MHz, The arbitrarily-selected bunch length corresponds to a frequency of 100 MHz plus $20.1/(2\pi)$.

5.3 Signal to Noise Ratio

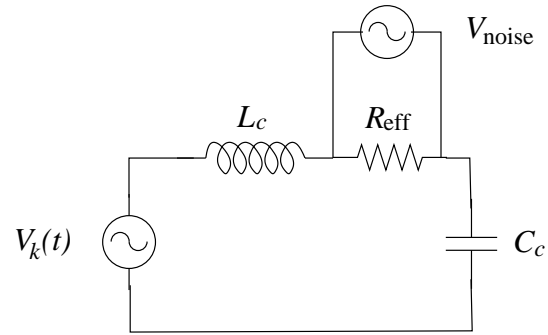


Figure 12: Circuit model for the polarimeter resonator excited by the polarized beam magnetization.

| parameter name | parameter symbol | formula | unit | value |
|-----------------------|------------------|--|--------|------------------------|
| length | l_c | | m | 0.5 |
| radius | R_c | | cm | 1 |
| gap/dielec.const. | g_c/ϵ_r | | micron | 1 |
| thickness | w_c | | mm | 5 |
| capacity | C_c | $\epsilon_0 \frac{w_c l_c}{g_c/\epsilon_r}$ | nF | 22.1 |
| inductance | L_c | $\mu_0 \frac{\pi R_c^2}{l_c}$ | nH | 0.790 |
| resonant freq. | f_c | $\frac{c}{2\pi^{3/2} R_c} \sqrt{\frac{g_c/\epsilon_r}{w_c}}$ | MHz | 38.1 |
| quality factor | Q_c | | | 10^{10} |
| eff. resist. | R_{eff} | $\frac{\omega_c L_c}{Q_c}$ | ohm | 1.89×10^{-11} |
| rev. freq. | f_0 | v/C_1 | MHz | 0.355 |
| res. harm. number | h_c | f_c/f_0 | | 107 |
| RMS bunch length | σ_b | σ_b | m | 1.2 |
| “natural” bunch freq. | f_b | $\frac{v}{4\sigma_b}$ | Mhz | 37.5 |

6 Beam-Beam Polarimetry



BOTH FAIL



BOTH SUCCEED



Figure 13: Two “pitchers” are throwing (special) balls toward each other, trying to make them “curve” in the natural direction of curve balls in baseball. Any success they have depends on collisions with balls coming in the opposite direction (and treated as viscous medium).

6.1 Polarimetry Counting Statistics

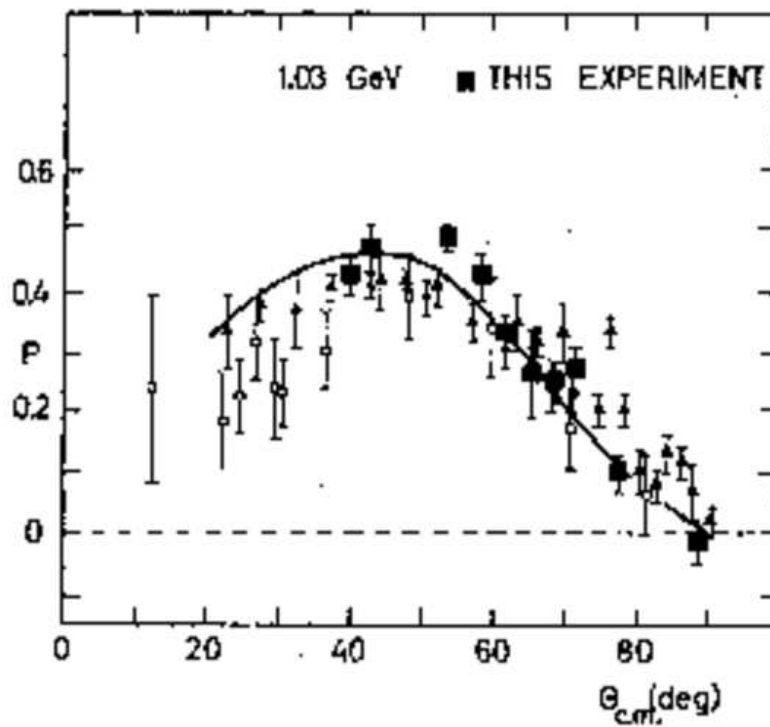


FIG. 8. Polarization in p - p scattering at 1.03 GeV. Open squares represent data from Ref. 15; shaded triangles, data from Ref. 3.

Figure 14: p - p polarization measurements of Neil, Longo et al. at the effective lab energy $K_{lab.} = 1.03$ GeV.

7 Storage Ring Options

7.1 Number of Bunches in Each Beam

- Carbon polarimetry favors multiple, alternately polarized bunches.
- Beam-beam polarimetry favors one bunch per beam (for best luminosity).
- Resonant polarimetry demands one bunch per beam (because of poor time resolution).

Table 1: Parameters for various storage ring options. All parameters (except in the last row) are specific to rings and independent of polarimetry and RF cavity parameters. Bold face entries correspond approximately with numerical examples in the text.

| polarimetry | | | BNL, carbon | | FNAL, resonant | |
|---------------------------|---|---------------|-------------|-----------|------------------|-----------|
| | | | intensity | | intensity | |
| quantity | symbol | unit | low | high | low | high |
| circumference | \mathcal{C}_0 | m | 263.4 | 263.4 | 506.7 | 506.7 |
| period | T_0 | μs | 1.46 | 1.46 | 2.82 | 2.82 |
| rev. freq. | f_0 | MHz | 0.683 | 0.683 | 0.355 | 0.355 |
| protons per bunch | N_p | | 2.0e8 | 1.0e9 | 1.0e10 | 1.0e11 |
| bunches in each ring | N_B | | 24 | 24 | 1 | 1 |
| bunch length | σ_z | m | 0.1 | 0.2 | 1.2/4.8 | 12.0 |
| beta functions at IP's | β_x^*/β_y^* | m | 28/240 | 28/240 | 0.31/0.72 | 0.31/0.72 |
| beta function maxima | $\beta_x^{\text{max}}/\beta_y^{\text{max}}$ | m | 28/240 | 28/240 | 80/200 | 80/200 |
| tunes | Q_x/Q_y | | 1.30/0.20 | 1.30/0.20 | 5.76/7.20 | 5.76/7.20 |
| beam-beam tune shift | ξ | | -1.6e-3 | -0.8e-2 | -0.0033 | -0.033 |
| Laslett tune shift | $\Delta Q_{\text{Laslett}}$ | | 0.036 | 0.090 | 0.046 | 0.185 |
| p-p collision rate per IP | | 1/s | | | 19/9.5 | 190/95 |
| resonant S/N | $V_k/\sqrt{V^2}$ | | | | 70.6 | 706 |

8 Measuring p and ${}^7\text{Li}$ EDM's in the Same Ring

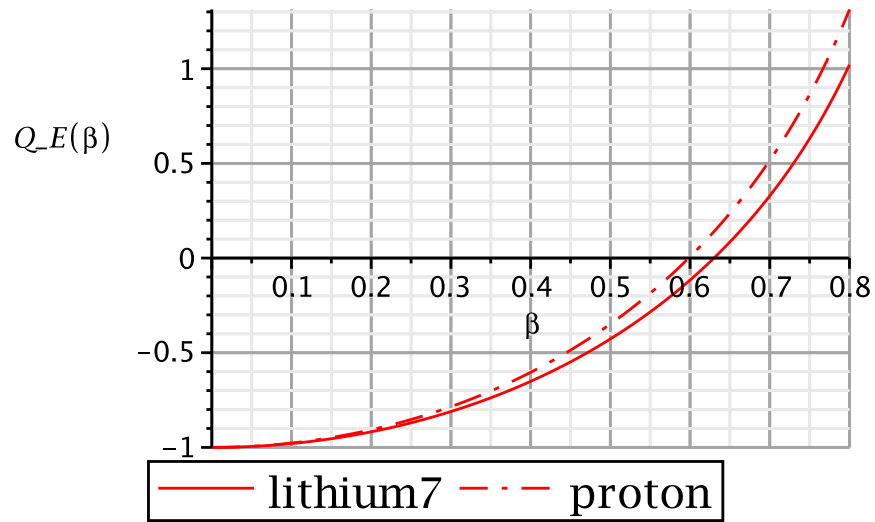


Figure 15: Electric field spin tune as function of particle speed for proton and ${}^7\text{Li}$.

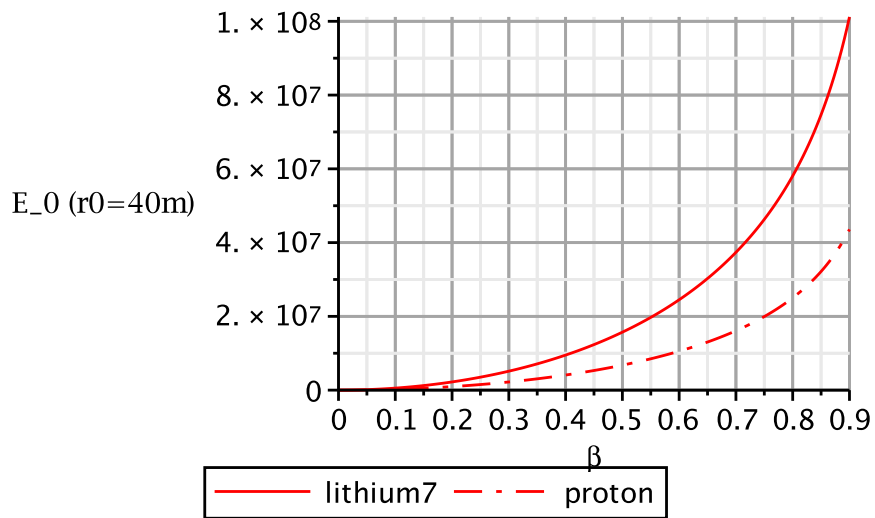


Figure 16: Storage ring electric field value required for proton and ${}^8\text{Li}$, in a ring with radius $r_0 = 40$ m.

- 9 (Precisely-) Fixed Frequency Feed-Forward Storage Ring Operation (as Contrasted with Polarimeter-RF Feedback)
- RF frequency is set to its nominal phase and amplitude, close to matching T_0 (which is only approximately known). f_{rf} is to be held perfectly fixed during any single run.
 - Beam is injected from one of the injection lines; some is captured in RF buckets but soon spirals in or out and is lost.
 - Electric field is adjusted to eliminate the spiraling. This setting is then further stabilized by FEEDBACK FROM RADIAL BEAM POSITION TO ELECTRIC FIELD.
 - Captured beam is steered onto the design orbit with exquisite accuracy, say $\pm 0.5 \times 10^{-4}$ m accuracy, using radial BPM's and radial kickers. At this point, from f_{rf} and known harmonic number, T_0 is known to arbitrary accuracy and C_0 is known to 10^{-7} fractional accuracy.

- All parameters can then be adjusted to move the proton speed onto its magic value with $\pm 10^{-7}$ fractional accuracy. In this state the polarization can be expected, typically, to precess through one full revolution roughly every 10^7 turns; that is, every 10 s.
- Using peripheral connection electronics, the resonant polarimeter frequency has meanwhile been tuned onto the nominally correct harmonic of the RF frequency. Fully polarized beam is then injected. Especially with multiple polarimeters and multiple tries, this should give a hint of signal in the resonant polarimeters.
- From this point, using FEED-FORWARD FROM THE RESONANT POLARIMETER, the RF frequency is adjusted onto the precise frozen spin frequency.

- As long as the beam polarization does not decay, since the relative tuning of RF and resonator is known to be approximately correct, one expects the resonator response to fade in and out in response to unpredictable drifts. In the absence of noise, with no drifts, one would OBSERVE BEATS SHOWING THAT THE BEAM POLARIZATION IS ALMOST, BUT NOT PRECISELY, FROZEN.
- This situation would still not be satisfactory since any EDM effect would average to zero even if the total precession is only through 2π . To have any hope of detecting an EDM signal the beams have to be perfectly frozen. With ZERO BEATS the EDM effect can accumulate indefinitely.
- **BOTTOM LINE: THE ABSENCE OF “BEATS” IN RESONATOR RESPONSE IS PROOF-POSITIVE OF FROZEN SPIN POLARIZATION THROUGH THE WHOLE RUN.**

9.1 Readout

- Readout from the resonant polarimeter can resemble the readout from cryogenic, resonant KID (kinetic induction detectors), recently invented for measuring CMB (cosmic microwave background).
- KID can (in principle) detect (the energy deposited by) single soft photons in each of thousands of channels.
- We have to detect (the magnetic moment of) 10^{10} protons in several units.

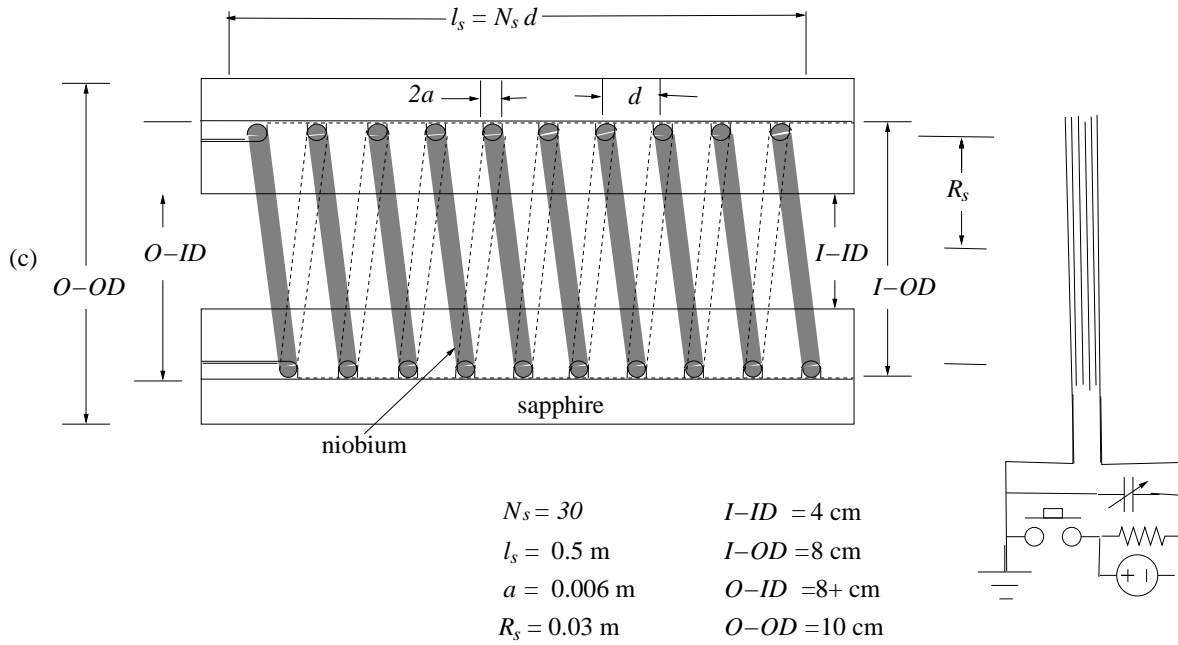


Figure 17: Possible resonator readout circuit.

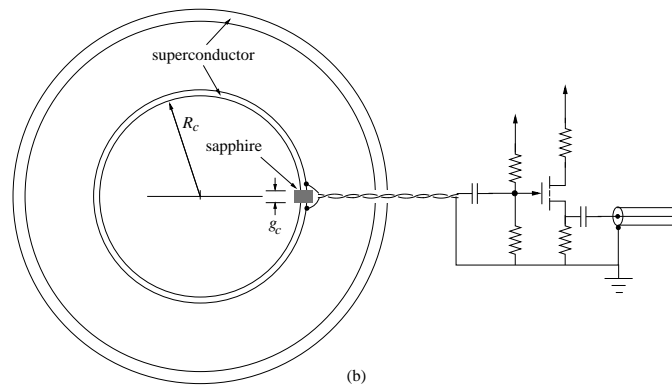


Figure 18: (b) End view of polarimeter and readout (copied from reference Huan et al. and using a low temperature pHEMT transistor such as Agilent type ATF-35143 in a source follower circuit).